Biofunctional magnetic nanoparticles for protein separation and pathogen detection

Hongwei Gu,†[a] Keming Xu,[b] Chenjie Xu‡[a] and Bing Xu*[b]

Received (in Cambridge, UK) 5th October 2005, Accepted 30th November 2005
First published as an Advance Article on the web 19th January 2006
DOI: 10.1039/b514130c

Recent successful syntheses of monodispersed magnetic nanoparticles have offered a unique opportunity to control and probe biological interactions using magnetic force. This paper highlights a general strategy to generate biofunctional magnetic nanoparticles, illustrates applications for these nanoparticles in protein separation and pathogen detection, and analyzes the high sensitivity and high selectivity achieved by this system.

[a]*Department of Chemistry, The Hong Kong University of Science and Technology, Clear Water Bay, Hong Kong, China*
[b]*Bioengineering Program, The Hong Kong University of Science and Technology, Clear Water Bay, Hong Kong, China.*
E-mail: chbingxu@ust.hk; Fax: +852 2358 1594; Tel: +852 2358 7351
† Present address: Department of Chemistry, Massachusetts Institute of Technology, Cambridge, MA 02139, USA.
‡ Present address: Department of Chemistry, Brown University, Providence, RI 02912, USA.

Hongwei Gu received his BSc and MSc in Chemistry from the Department for Intensive Instruction (1998) and Department of Chemistry (2001) at Nanjing University, respectively. He obtained his PhD in 2004 from The Hong Kong University of Science and Technology under the supervision of Dr Bing Xu. At present, he is a postdoctoral associate in the Department of Chemistry & Institute of Soldier Nanotechnologies at M. I. T. with Professor Timothy Swager. His current research focuses on carbon nanotube-based actuation materials.

Keming Xu is currently pursuing a PhD degree in bioengineering at The Hong Kong University of Science and Technology. He received his bachelor's degree from the Department of Biochemistry at Nanjing University. His research interest is focused on the application of nanoparticles in protein interactions and the development of hydrogels as biomaterials.

Chenjie Xu received his BSc in Chemistry at Nanjing University in 1998. He is currently pursuing a PhD degree in Chemistry at Brown University after receiving an MS in chemistry from The Hong Kong University of Science and Technology.

Bing Xu received his BS and MS from Nanjing University in 1987 and 1990. He obtained his PhD in 1996 from the University of Pennsylvania under the supervision of Timothy Swager. From 1997 to 1999, he was an NIH postdoctoral fellow with George Whitesides at Harvard University. Professor Xu joined The Hong Kong University of Science and Technology in Aug. 2000, and he is now an Assistant Professor of Chemistry. He is the recipient of the DuPont Asian & European Young Investigator Award (2001). His research focuses on the applications of supramolecular chemistry to materials, nanoscience, and biological science.

Introduction

In the past two decades, our understanding of molecular biology, genomics, and nanotechnology has expanded explosively. The inevitable intersection of these three disciplines has set in motion the development of an emerging research area, bionanotechnology or nanobiomedical technology, which offers exciting and abundant opportunities for discovering new processes, phenomena, and science. In particular, the advances in the synthesis and characterization of nanoscale materials[1–7] allow scientists to understand and control the interactions between nanomaterials (*e.g.*, nanowires, nanofibers, nanoparticles, nanobelts or nanoribbons, and nanotubes) and biological entities (*e.g.*, nucleic acid, proteins, or cells) at molecular or cellular levels. These advances promise major achievements in the life sciences.[8] For example, Mirkin *et al.* reported that a target DNA induces sequence-specific nanoparticle aggregation and changes the color of the solution.[4,9] This simple phenomenon led to the development of a DNA detection assay based on gold nanoparticles.[9] This example illustrates the far-ranging potentials of using nanomaterials in biodiagnostics. It stimulated worldwide research interest in developing nanomaterial-based bioanalytical techniques. Like gold nanoparticles, quantum dots, which have exceptional optical properties (*e.g.*, broad excitation spectra, sharp emissions, and quench-resistance), have attracted intensive research efforts and are replacing conventional organic fluorescent dyes in bioassays (*e.g.*, multiplexed DNA detection or tumor imaging).[10] Despite the clinical success of using iron oxide as a magnetic resonance imaging (MRI) contrast agent (for enhancing the T_2 relaxation times), magnetic nanoparticles have not been used in many biological applications, unlike gold nanoparticles and quantum dots. This lack of interest in magnetic nanoparticles is partly due to difficulties in making monodispersed magnetic nanoparticles and their lack of a robust chemistry for surface functionalization.

The recent successful syntheses of monodispersed magnetic nanoparticles,[1–3,11] though originally intended to be used in high density magnetic storage media, provide a basis on which to explore further applications of magnetic nanoparticles in biomedicine. In fact, several groups demonstrated exciting and promising biological applications of magnetic nanoparticles.

For example, Weissleder *et al.* showed that magnetic nanoparticles can be used in MRI for monitoring specific enzymes and detecting viruses.[12] Cheon *et al.* reported the use of multifunctional magnetic nanocrystals to detect cancer *in vivo*.[13] Willner *et al.* demonstrated that magnetic nanoparticles can act as a magnetoswitch to induce selective bioelectrocatalysis, detect cancer, and amplify DNA detection.[14] The above studies and other explorations[15] verify the potential of magnetic nanoparticles in life science, as summarized in several authoritative reviews.[16]

This paper describes the general principles of the design and synthesis of biofunctional magnetic nanostructures and reviews several key issues (*e.g.*, size, composition, surface modification, and complexity) that are related to the capture of cells[17,18] and separation of proteins.[19,20] After discussing the size and composition of magnetic nanoparticles, we describe the surface chemistry of functionalizing magnetic nanoparticles. Then, we demonstrate the advantages of magnetic nanoparticles in protein separation and bacteria capture. Finally, we discuss some potential candidates of biofunctional magnetic nanoparticles and offer a brief summary and outlook.

Size and composition of biofunctional magnetic nanoparticles

The recent advances in synthesis offer the capability to control precisely the size of magnetic nanoparticles from 2 to 20 nm in diameter.[2] This capability may allow the size of particles to be application specific or target specific. Fig. 1 illustrates the relative sizes of molecules, nanoparticles, and common biological targets. Two simple principles can be used for choosing the optimal size of biofunctional magnetic nanoparticles to achieve high affinity, high selectivity, and high sensitivity in interaction with targeted biological moieties: (1) the size should be large enough to allow the presence of multiple ligands on the particle surface to achieve multivalent interactions; (2) the size should be small enough to yield high surface-to-volume ratios, good colloidal stability, and fast movement for high binding rates. Specifically, in the separation of proteins, the sizes of the nanoparticles should be comparable to the size of biomacromolecules; in the capture of cells, the size of the nanoparticle should be 8 to 10 nm in diameter.

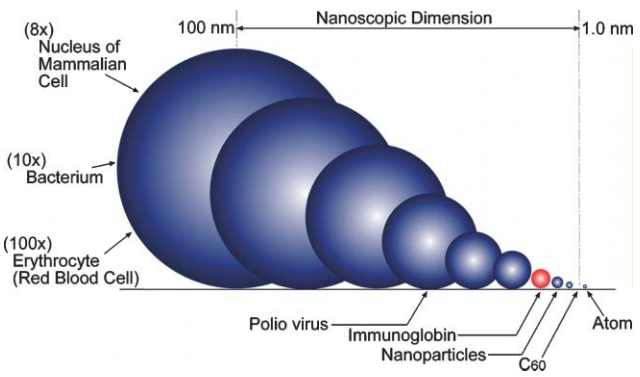

Fig. 1 Comparison of the sizes of atoms, nanoparticles, and biological entities.

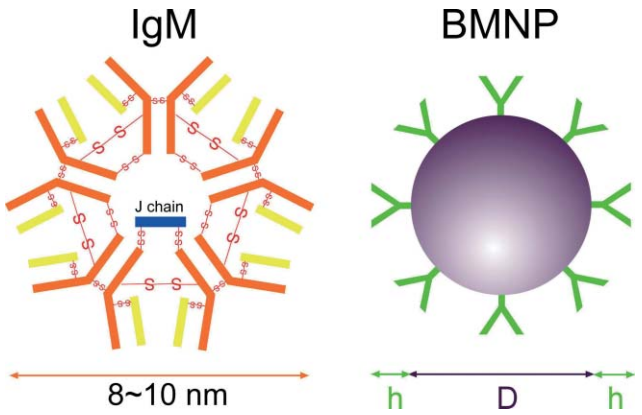

Fig. 2 The finite size (8–10 nm) of $(IgM)_5$ and the height (h) of the ligands and the core diameter (D) of a biofunctional magnetic nanoparticles (BMNP).

The choice of 8 to 10 nm particle diameters is based on the high avidity in cell binding events exhibited by immunoglobulin M pentamer ($(IgM)_5$, whose finite size is 8 to 10 nm). As postulated in Fig. 2, when ligands or receptors are decorated appropriately on the surface of a magnetic nanoparticle, in terms of multivalent binding, the particle may act as an artificial $(IgM)_5$ or a "magnetic artificial antibody". That is, it may bind to a target cell with high or maximum valence under optimal conditions. This kind of biofunctional magnetic nanoparticle ($D + 2h$ = 8 to 10 nm) might provide the highest possible selectivity and sensitivity.

Besides having the proper size (*i.e.*, 8–10 nm), biofunctional magnetic nanoparticles have to satisfy other prerequisites, including stability, biocompatibility, and biodegradability. For *in vivo* applications, biofunctional magnetic nanoparticles must meet all three of these prerequisites. If they are used for *in vitro* applications, good chemical stability is necessary and adequate. For the applications described here, the magnetic nanoparticles also need to have large saturation magnetization (M_s) in order to be manipulated by a magnetic force, which leaves only a handful of possible candidates (*e.g.*, Ni, Fe, Co, FePt, FePd, CoPt, MnAl, $SmCo_5$, and $Fe_{14}Nd_2B$).[21] Among these materials, nickel, iron, or manganese aluminium alloy nanoparticles would be unusable without protecting layers, and $Fe_{14}Nd_2B$ nanoparticles remain a synthetic challenge. Therefore, FePt becomes the material of choice to construct biofunctional magnetic nanoparticles because of its chemical stability and large M_s.[1] In our studies on the chemical synthesis of $SmCo_5$ magnetic nanoparticles,[6] we found that core–shell structured $Co@Fe_2O_3$ or $SmCo_{5.2}@Fe_2O_3$ magnetic nanoparticles are also useful for making biofunctional magnetic nanoparticles.[19]

Anchoring biofunctional molecules onto magnetic nanoparticles

There are three general ways to connect biofunctional molecules to the surface of a nanoparticle. The well-established method is to coat the nanoparticle with polymers, and then form covalent bonds between the polymer coating and the biofunctional molecules. Although widely used, polymer

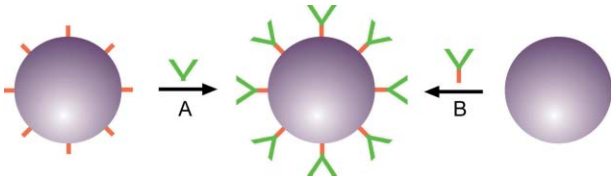

Fig. 3 Two ways to attach biofunctional molecules to a nanoparticle (the red fragment represents the surface anchor).

coating often leads to nonspecific absorption of other substances than the desired targets, which decreases the selectivity that is critical for protein separation or capture of cells. Therefore, we focus our discussion on the two other methods as shown in Fig. 3. In route A, a monolayer of molecules that bear a reactive group grows on the nanoparticles first; then, the biofunctional molecules react with the monolayer to yield the biofunctional nanoparticles; in route B, the group that reacts with the surface is conjugated with the biofunctional molecule first; then, the conjugate reacts with the nanoparticle to give the desired product. Route A is simple and versatile, but may leave unconsumed reactive groups; route B produces a well-defined monolayer, but it sometimes requires considerable effort to engineer a biofunctional molecule that bears a surface reactive group.

Success from both routes A and B has been reported.[7,17,18,22,23] For example, following route A, Abad *et al.* recently devised a simple reaction strategy (Fig. 4a) to construct nitrilotriacetate group (NTA)-terminated gold nanoparticles.[24] After being synthesized in toluene by the two-phase reduction of aqueous $HAuCl_4$ using tetra-*n*-octylammonium bromide (TOABr) as the phase transfer agent, gold nanoparticles (3–4 nm) were derivatized by reacting them with 6,8-dithioctic acid. The carboxylic acid-terminated gold nanoparticles are then redispersed in an aqueous solution to react with an amino-nitrilotriacetic–Co(II) complex to yield **3**. On the basis of elemental analysis, the authors reported that the surface coverage by sulfur atoms on **1** close to a reported monolayer of thiolate surface was 7.6×10^{-10} mol cm^{-2} on Au(111), suggesting that the formed monolayer is of excellent quality. The coverage of Co–NTA (**2**) on gold nanoparticles, however, has yet to be established.

Our synthesis of nitrilotriacetic acid (NTA)-modified magnetic nanoparticles[19,20] follows route B. As shown in Fig. 4b, with magnetic nanoparticles composed of FePt alloy, the thiol acts as the anchoring group for NTA because the Pt–S and Fe–S bonds form in high yields and are relatively strong and stable. To convert NTA into **5**, the thiol group protected by mercaptoalkanoic acid is activated with *N*-hydroxysuccinimide first and then react with N_α,N_α-bis(carboxymethyl)lysine to give **5** after deprotecting the thiol group. FePt nanoparticles react with **5** to form Pt–S and Fe–S bonds that link **5** to FePt. After reacting with excess $NiCl_2 \cdot 6H_2O$, the water stable product **6** is easily separated from the organic phase. The UV–vis spectra of the aqueous solution of **6** indicate that **5** attaches to the FePt nanoparticles. X-Ray photoelectron spectroscopy (XPS) of **6** shows the formation of Fe–S and Pt–S bonds. Transmission electron micrographs (TEM) indicate that the morphology of **6** changes

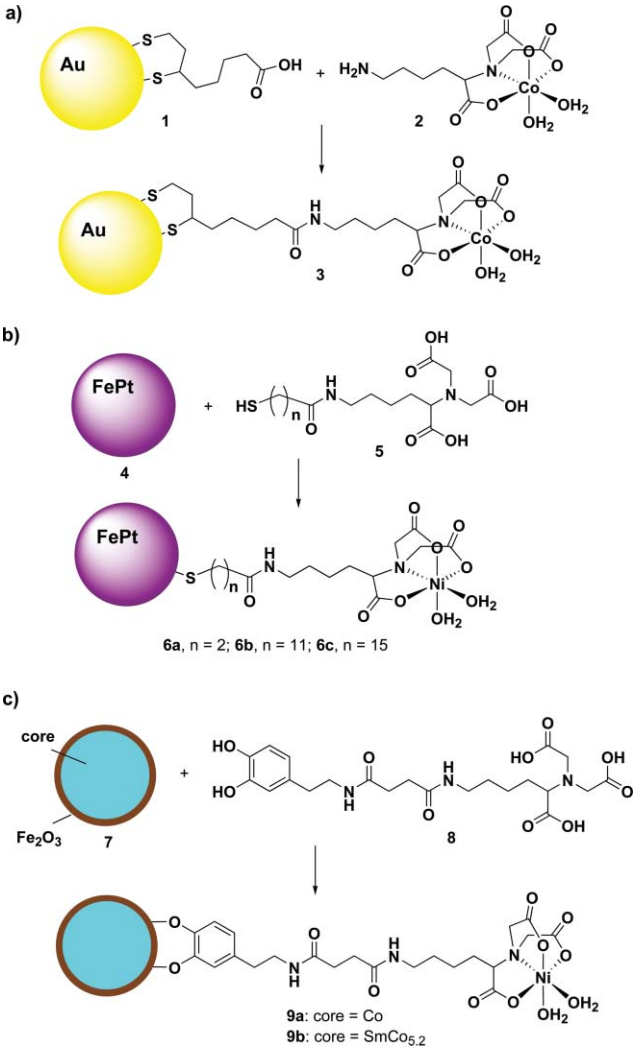

Fig. 4 The reaction route for the construction of (a) NTA-terminated gold nanoparticles (**3**); (b) NTA-terminated FePt magnetic nanoparticles (**6**); and (c) NTA-terminated core–shell magnetic nanoparticles (**9**).

little except for slightly increased aggregation after **5** binds to the FePt nanoparticles. Magnetic measurements reveal the superparamagnetic behavior of **6**, which allows **6** to be attracted by a small magnet. We also find that **6b** and **6c** have 108 and 75 NTAs on the particle surface, respectively.

For magnetic nanoparticles composed of Fe_2O_3 shell and Co or $SmCo_{5.2}$ core, we have to develop a new surface anchor to connect NTA to the iron oxide shell because there is no reliable and robust established chemistry to form organic monolayers on iron oxide. Because spectroscopic study[25] suggests that bidentate enediol ligands, such as catechol, form tight bonds with iron oxide by converting the under-coordinated Fe surface sites back to a bulk-like lattice structure with an octahedral geometry for oxygen-coordinated iron, we link dopamine (DA) to NTA for anchoring DA–NTA onto iron oxide. After its hydroxyl groups are protected with benzyl bromide, dopamine reacts with succinic acid anhydride to transform the amine end into a carboxylic acid, which further reacts with N_α,N_α-bis(carboxymethyl)lysine to give **8** after

deprotecting the hydroxyl groups. Co (or $SmCo_{5.2}$)@Fe_2O_3 nanoparticles react with **8** to form Fe–O bonds that link **8** to the Fe_2O_3 shell. The resulting product reacts with $NiCl_2{\cdot}6H_2O$ to give **9** in the aqueous phase (Fig. 4c). Spectroscopic characterizations prove that **8** is covalently attached to the surface of Fe_2O_3. Magnetic measurements reveal the superparamagnetic behavior of **9**, and the saturated magnetizations are sufficient to allow **9** to be attracted by a small magnet. We find that about 27 and 50 molecules of **8** respectively cover each Co@Fe_2O_3 and $SmCo_{5.2}$@Fe_2O_3 nanoparticle. In addition, a thermal stability test confirms that **9b** remains functional even after being boiled in water.

Recently, Rotello *et al.*[26] reported the formation of mixed monolayers on FePt magnetic nanoparticles using thiol and dopamine-terminated poly(ethyleneglycol) (PEG). They showed that the surface thiol PEG is exchangeable with smaller thiol compounds. Using other thiols to replace PEG, the authors created FePt nanoparticles with partially covered surface of either positively charged ammonium ions or negatively charged carboxylates. The resulting functionalized FePt nanoparticles exhibited good stability in water and displayed expected binding with charged biomolecules. This reported procedure combines routes A and B and illustrates another general strategy to produce functionalized FePt nanoparticles.

To develop biofunctional magnetic nanoparticles for capturing bacteria at ultralow concentrations, we use thiolated vancomycin (Van, **10**)[27] to react with FePt nanoparticles. We choose Van as the ligand because Van binds to the terminal peptide (D-Ala-D-Ala, **11**) on the cell wall of a Gram-positive [G(+)] bacterium *via* hydrogen bonds (Fig. 5a), and previous studies have demonstrated that multivalent Vans have high affinities toward bacteria when Van is presented on a rigid platform.[23,28] As illustrated in Fig. 5b, bis(vancomycin) cystamide (**12**)[27] (in aqueous solution) reacts with FePt nanoparticles (in hexane phase) to form **13**, a water stable product that is easy to separate from the organic phase (Fig. 5c). FePt nanoparticles also react with cystamine (**14**) to give water stable FePt–NH_2 (**15**) as a control compound. There are 1800 molecules of **14** covering the surface of **15**, and 8 or 9 Vans covering **13**.[17]

Protein separation using biofunctional magnetic nanoparticles

Effective manipulation of proteins is important to studies and applications in the life sciences. Particularly in proteomics, the purification of native or recombinant proteins is a time-consuming routine. The successful synthesis of NTA-terminated magnetic nanoparticles offers a simple and versatile platform for protein separation. Obviously, magnetic nanoparticles (8 to 10 nm) should perform better than micron-sized resins or beads used in metal–chelate affinity chromatography (MCAC) because their high surface-to-volume ratio, fast movement, and good dispersability result in a higher binding rate between the Ni–NTA and histidine-tagged proteins. The high surface-to-volume ratio also increases the protein binding capacity of the nanoparticles. In addition, the high binding rate has a subtle advantage. The target proteins cover the

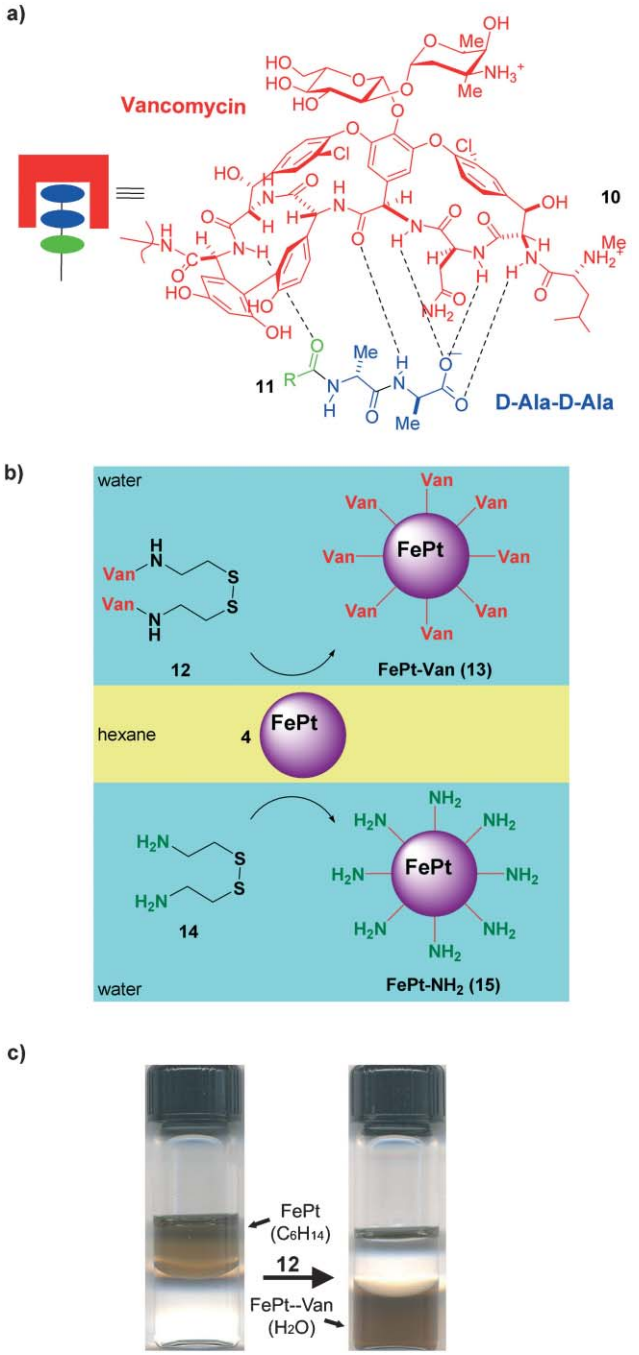

Fig. 5 (a) The structure of vancomycin; (b) the simple biphasic reaction to attach vancomycin to FePt magnetic nanoparticles, and (c) the optical image of **4** in hexane and **13** in water.

surface of the nanoparticles quickly, thus rapidly reducing the overall unoccupied surface area that may be available for non-specific absorption of proteins. Therefore, the nanoparticles achieve much higher specificity than do microparticles. Moreover, the use of NTA-terminated magnetic nanoparticles eliminates the pretreatment of the cell lysate because a magnet easily separates the target proteins (Fig. 6a).

As shown in Fig. 6b, the general procedure for using NTA-terminated magnetic nanoparticles for protein separation consists of three simple steps: 1) adding NTA-terminated

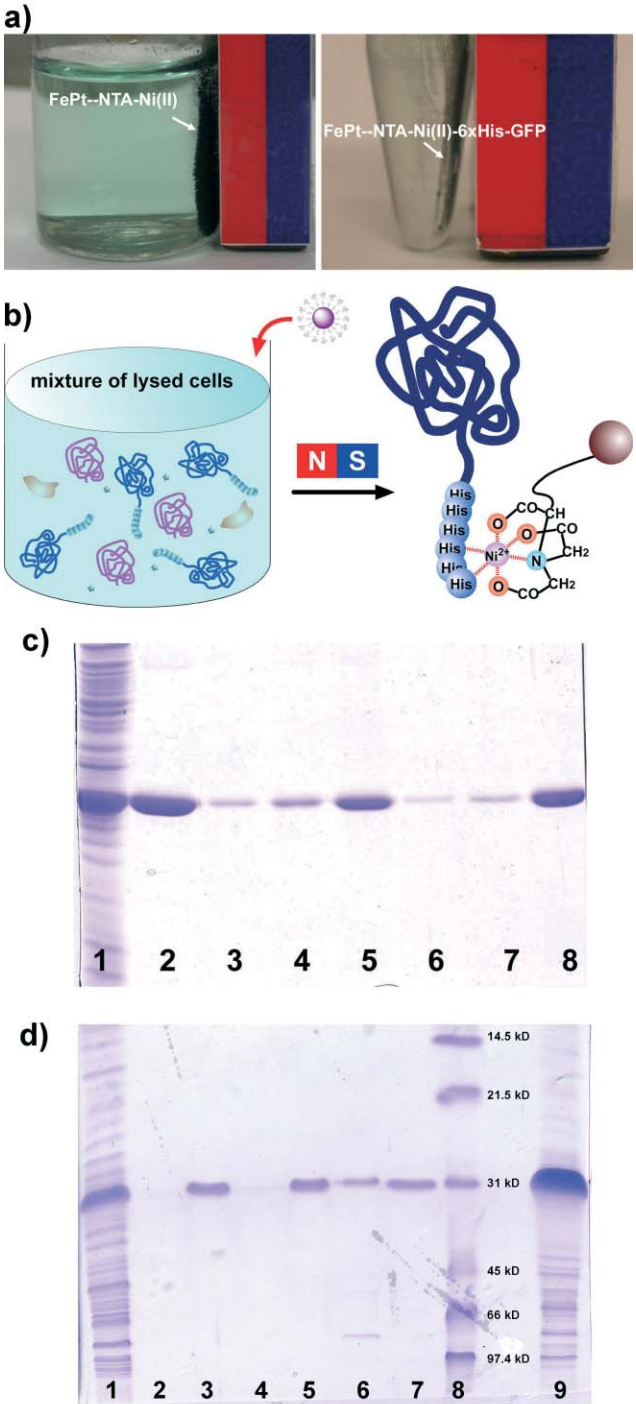

Fig. 6 (a) Optical images of a magnet attracting **6c** and **6c**-6xHis-GFP; (b) surface-modified magnetic nanoparticles selectively binding to histidine-tagged proteins in a cell lysate; (c) SDS/PAGE analysis of the cell lysate (lane 1), the fraction (lane 2) washed off a commercial Ni^{2+}–NTA column; the fraction washed with the freshly made **6c** using imidazole solution (10 mM, lane 3; 80 mM, lane 4; 500 mM, lane 5); fractions washed off the reused **6c** using imidazole solution (10 mM, lane 6; 20 mM, lane 7; 500 mM, lane 8); and (d) the cell lysate (lane 1), the molecular weight marker (lane 8), the fractions washed from the freshly made **9b** (lanes 2 and 3), boiled **9b** (lanes 4 and 5), and the commercial HiTrap affinity column (lanes 6 and 9), and the concentrations of imidazole are 10 mM (lanes 2, 4, and 6) and 500 mM (lanes 3, 5, 9).

magnetic nanoparticles into the suspension of the lysed cells and shaking for five minutes; 2) using a small magnet to attract the nanoparticles to the wall of the vial and washing them with de-ionized water to remove any residual protein solution; and 3) using a concentrated imidazole solution to wash the nanoparticles to yield pure histidine-tagged proteins. After releasing the proteins and being washed sequentially by EDTA, the buffer solution, the $NiCl_2{\cdot}6H_2O$ solution, the NTA modified magnetic nanoparticles can be recovered and reused without losing efficiency and capacity.

Analyses of the purity of the histidine-tagged protein (*i.e.*, 6xHis-GFP) separated by the magnetic nanoparticles confirm the high specificity provided by the nanoparticles. The elutions (obtained by sequentially washing **6c** with 10 mM, 80 mM, and 500 mM imidazole solutions) contain only 6xHis-GFP (Fig. 6c: lanes 3, 4, and 5). In addition, the affinity and specificity of **6c** remain unaffected after being recovered and reused (Fig. 6c: lanes 6–8). The binding capacity reaches 2 to 3 mg of protein/per mg of **6c**, which is about 200 times higher than that of commercially available magnetic microbeads (10 to 12 μg protein/1 mg bead). The lowest concentration of protein that could be separated by **6c** is about 0.33 nM. The Ni–NTA modified core–shell magnetic nanoparticles, **9b**, also show excellent specificity, as indicated by a test of thermal stability of **9b** and a comparison with a commonly used commercial product. After being boiled in Tris buffer for 15 min, the specificity and efficiency of **9b** remain unaffected. Electrophoresis traces show that the fraction washed from the boiled **9b** (Fig. 6d: lane 5) contains only the histidine-tagged protein, the same as the fraction washed from the freshly made **9b** (Fig. 6d: lane 3). Under the same conditions, the fraction washed from the commercial column (Fig. 6d: lane 6) still has two protein bands; in the final washing using a concentrated imidazole solution, the fraction from the column (Fig. 6d: lane 9) contains many other proteins. Thus, the specificity of **9b** for histidine-tagged proteins is obviously higher than that of the commercial HiTrap affinity column.

The specificity of the magnetic nanoparticles exhibited in protein separation suggests that magnetic nanoparticles, as a general and versatile system, should bind with other biological targets at low concentrations and with high specificity.

Pathogen detections using biofunctional magnetic nanoparticles

Instant and ultra-sensitive detection of pathogens (*e.g.*, bacteria, viruses) without time-consuming procedures, such as incubation or amplification by polymerase chain reaction (PCR), offers obvious clinical benefits. However, there has been no general and satisfactory assay that detects bacteria at concentrations of less than 10^2 cfu mL^{-1} without pre-enriching bacteria *via* an inoculation process. Using our biofunctional magnetic nanoparticles, **13**, we are able to capture and detect of a wide range of bacteria at concentrations of less than 10^2 cfu/mL within an hour. After mixing **13** with a solution of a bacterium for about 10 minutes, a point magnet easily attracted the bacteria whose cell surfaces was bound with **13**. The bacteria and **13** formed aggregates under the magnetic

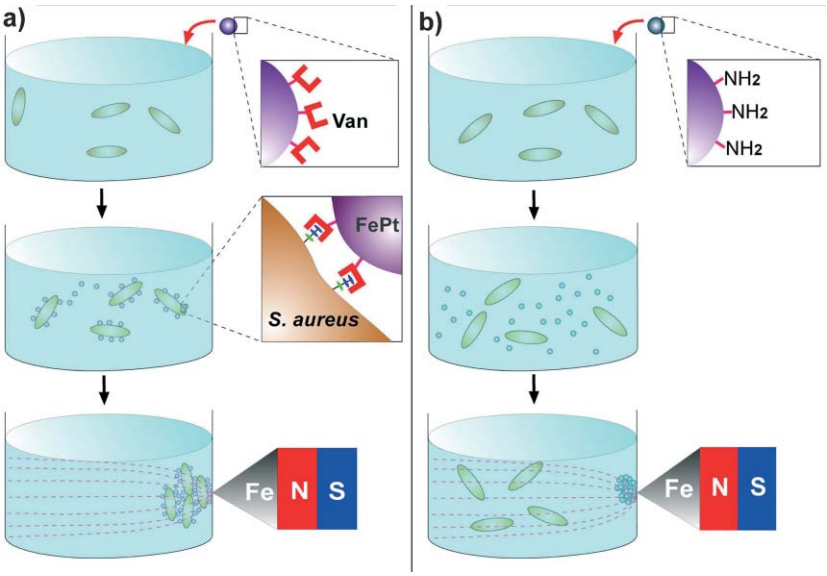

Fig. 7 (a) **13** capturing bacteria *via* a plausible multivalent interaction and (b) the corresponding control experiment (Reproduced with permission from ref. 17. Copyright 2003 American Chemical Society).

force. The same procedure was carried out using **15** as the control (Fig. 7).

Because of the distinct differences in sizes between nanoparticles and bacteria, a scanning electron microscope (SEM) easily distinguishes the bacteria from the aggregates (Fig. 8). We found that **13** indeed captures bacteria strains, while **15** fails to bind to any bacteria.[17] As summarized in Table 1, **13** captured *S. aureus* at 8 cfu mL^{-1}, *S. epidermidis* at 10 cfu mL^{-1}, coagulase negative staphylococci (CNS) at 4 cfu mL^{-1}, *E. faecalis* (ATCC 29212) at 26 cfu mL^{-1}, and *E. coli* at 15 cfu mL^{-1}. Although the affinity of Van with the terminal peptides on the cell wall of vancomycin resistant enterococci (VRE) decreases due to mutation, our previous study showed that Van-decorated gold nanoparticles[23] bound strongly to VRE. Similarly in the capture experiment, **13** captured VRE strains at concentrations of 10^1 to 10^2 cfu mL^{-1} (Table 1), likely due to multivalent interactions.

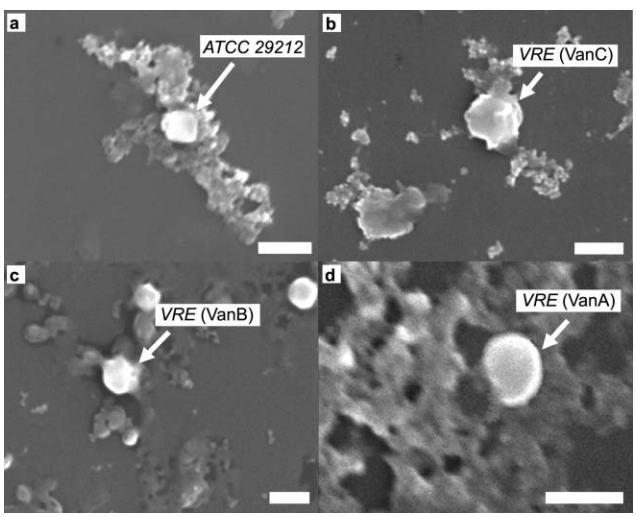

Fig. 8 SEM images of (a) *E. faecalis* (ATCC 29212, a Van sensitive strain, 26 cfu mL^{-1}); (b) *E. gall* (a VanC strain, 84 cfu mL^{-1}); (c) *E. faecium* (a VanB strain, 22 cfu mL^{-1}); and (d) *E. faecium* (a VanA strain, 34 cfu mL^{-1}) and the aggregates of FePt–Van (scale bars = 1 μm, the genotypes of the strains were determined by PCR, and the exact counts of bacteria were confirmed by back titration) (Reproduced with permission from ref. 17. Copyright 2003 American Chemical Society).

Though the sensitivity achieved using magnetic nanoparticles is only comparable to that of assays based on PCR, this direct capture protocol is faster than PCR when the bacterium count is low. In addition, using biofunctional magnetic nanoparticles to capture bacteria is useful because there are circumstances when PCR is inapplicable. For example, PCR-based detection would be inaccurate in determining low counts of bacteria in human blood because free genomes of bacteria usually exist in the blood. Therefore, it is particularly significant that **13** binds selectively to *S. epidermidis* (15 cfu mL^{-1}) in the presence of white blood cells (WBC, 100 cfu mL^{-1}).[17] To determine the existence of bacteria in

Table 1 The lowest concentrations of bacteria captured by **13**

Exp. no.	Bacteria	Type	Read-out method	Concentration/ cfu mL^{-1}
1	*S. aureus*	G(+)	SEM	8
2	*S. epidermidis*	G(+)	SEM	10
3	*S. epidermidis*	G(+)	SEM	15[a]
4	Coagulase negative staphylococci	G(+)	SEM	4
5	Coagulase negative staphylococci	G(+)	FL[b]	6
6	*E. faecalis* (ATCC 29212)	G(+)	SEM	26[c]
7	*E. gall* (VanC)	G(+)	SEM	84[c]
8	*E. faecium* (VanB)	G(+)	SEM	22[c]
9	*E. faecium* (VanA)	G(+)	SEM	34[c]
10	*Streptococcus pneumoniae*	G(+)	FL[b]	4
11	*E. coli*	G(−)	SEM	15
12	*E. coli*	G(−)	FL[b]	10

[a] Mixed with white blood cells whose concentration is 100 cfu mL^{-1}. [b] FL = fluorescence microscope. [c] Concentrations lower than indicated have not been tested.

blood in a clinical settings, SEM is impractical. We are now developing assays that combine fluorescence and magnetic nanoparticles; our preliminary studies indicate that this combination can detect CNS at 6 cfu mL^{-1}, *Streptococcus pneumoniae* at 4 cfu mL^{-1}, and *E. coli* at 10 cfu mL^{-1} (Table 1).

Biofunctional magnetic nanoparticles are so versatile that they can couple with other analytical means for pathogen detection. Recently, Chen *et al.* reported combining biofunctional magnetic nanoparticles with matrix-assisted laser desorption/ionization mass spectrometry (MALDI-MS) to probe for pathogenic bacteria.[22] The authors fabricated biofunctional nanoparticles by attaching human immunoglobulin (IgG) onto the surfaces of magnetite nanoparticles. The IgG-modified Fe_3O_4 nanoparticles, which bind selectively to IgG-binding sites on the cell walls of pathogens, serve as affinity probes to capture targeted bacteria from sample solutions. MALDI-MS is used to create a read-out of the captured bacteria. Chen *et al.* were able to detect both *S. saprophyticus* and *S. aureus* at concentrations of 3×10^5 cfu mL^{-1} in aqueous sample solutions and *S. saprophyticus* at 3×10^7 cfu mL^{-1} in a urine sample. Using iron nanoparticles instead of the magnetite naoparticles and vancomycin instead of the IgG, the researchers reported the detection of both *S. saprophyticus* and *S. aureus* of 7×10^4 cfu mL^{-1} in a urine sample. These works indicate the advantages of vancomycin decorated magnetic nanoparticles over antibody-modified particles for the capture of bacteria.

Further applications of biofunctional magnetic nanoparticles

Besides their unique ability to isolate targets out of a mixture with high specificity and high sensitivity, biofunctional magnetic nanoparticles can act as affinity labels (similar to the conjugate of an antibody and a gold nanoparticle) to elucidate specific biological interactions in an electron micrograph. For example, it was puzzling to us that vancomycin-decorated magnetic nanoparticles bound to Gram-negative (G−) bacteria such as *E. coli* because the outer membrane, presumably, should block the binding between vancomycin and D-Ala-D-Ala. Are there receptors for vancomycin on the outer membrane of *E. coli* or are there defects on the outer membrane to let vancomycin bind to a few exposed D-Ala-D-Ala? A comparison of the TEM images of *E. faecium* (VanA) and *E. coli* captured by **13** offers a probable explanation. As shown in Fig. 9, the nanoparticles (**13**) are uniformly distributed and cover the entire surface of the *E. faecium* (VanA) cells, but **13** binds to spots on the surface of the *E. coli* cells. The distribution of **13** on the surfaces of the two types of cells hints that defects on the outer membrane of *E. coli* cause the binding of **13** to *E. coli*.

The ability of biofunctional magnetic nanoparticles to serve as tags for mapping ligand receptor interactions on a cell (*e.g.*, vancomycin binding with D-Ala-D-Ala) suggests that it is worthwhile to conjugate magnetic nanoparticles with other labels or tags to expand the read-out method beyond TEM or SEM. One attractive candidate as labels is quantum dots because of their excellent optical properties. Because the attachment of a single reactive group or molecule on either a magnetic nanoparticle or a quantum dot is improbable, it is rather difficult to use organic linkers to connect the magnetic nanoparticle directly with the quantum dot without cross-linking. Therefore, we have devised a simple strategy to construct a heterodimer of magnetic nanoparticles and quantum dots (Fig. 10a).[5] This heterodimer of two nanocrystals (**16**) retains the properties of its discrete parts (FePt and CdS). That is, the heterodimer exhibits both the superparamagnetic behavior of FePt and the fluorescence of CdS (Fig. 10b). It should be possible to decorate FePt with a bioactive molecule to produce a biofunctional heterodimer.

Another attractive label is silver nanoparticles because their surface-enhanced Raman spectroscopic (SERS) signal is extremely valuable for probing biological systems.[29] We have demonstrated a simple, efficient, and general method to form heterodimeric nanostructures of magnetite and silver[7] based

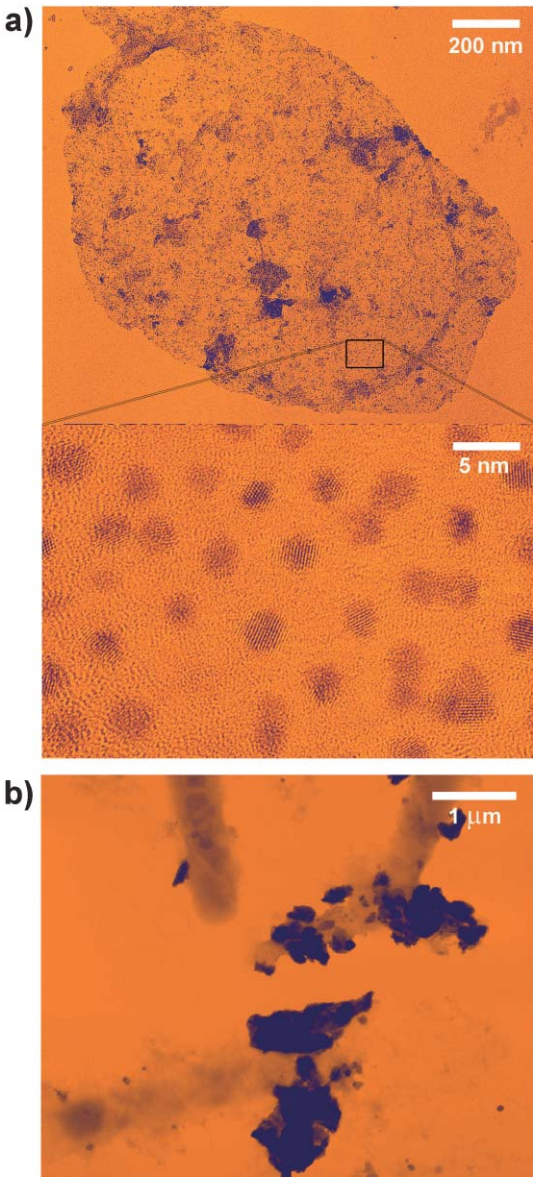

Fig. 9 TEM images of the bacteria captured by **13**: (a) *E. faecium* (VanA) and (b) *E. coli*.

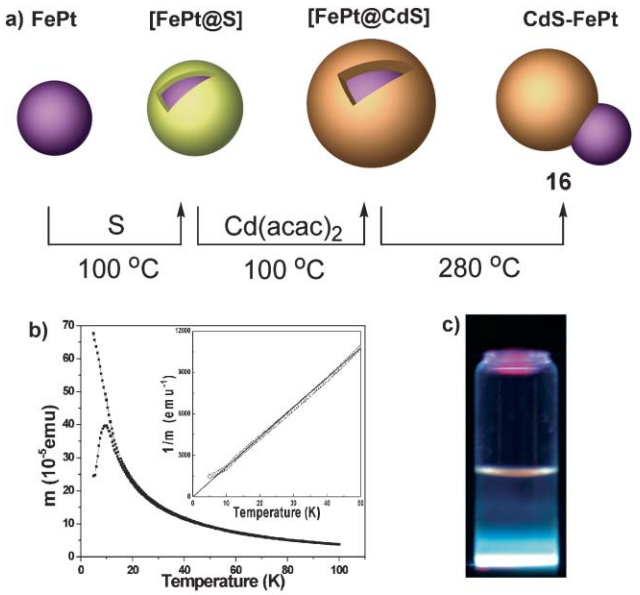

Fig. 10 (a) The typical synthetic route for making a heterodimer of magnetic nanoparticles and quantum dots; (b) temperature-dependent magnetization (ZFC/FC) measured with a magnetic field of 100 Oe (inset: FC, 1/*m* *vs.* *T*); and (c) a fluorescent image of the hexane solution of the heterodimer (**16**).

on a reaction at a liquid–liquid interface of colloidosomes.[30] This procedure not only controls the size and composition of the nanoparticle heterodimers, but it also allows functional molecules to attach on specific parts of the heterodimers. As shown in Fig. 11, two different functional molecules bind to the specific parts of the heterodimer (**17**) to produce a multifunctional heterodimer (**21**) that is hydrophilic, fluorescent, responsive to magnetic forces, and able to bind to specific receptors. We envisage that such heterodimers will be

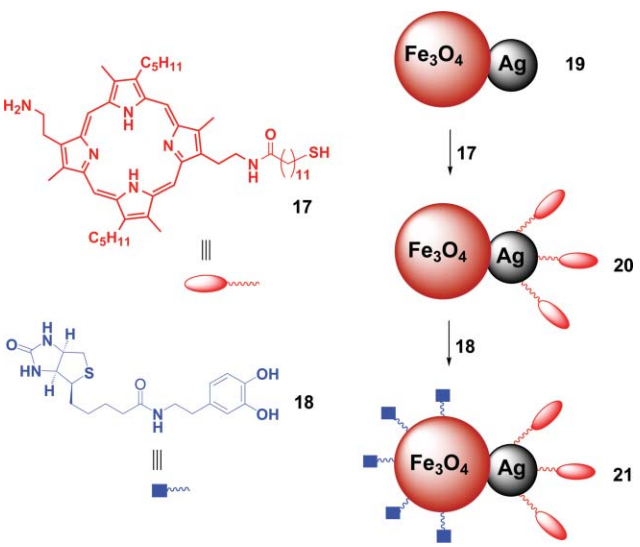

Fig. 11 The schematic synthetic route to engineer two different arrays of functional molecules with dimensions of less than 20 nm (Fe_3O_4: D = 8 nm; Ag: D = 5.5 nm).

useful nanomaterials in applications such as protein binding, molecular imaging, and pathogen detection.

Summary and outlook

In the last five years, research activities on magnetic nanoparticles have increased significantly. For example, according to the Web of Science, there are about 100 entries on magnetic nanoparticles from 1991–1999 and about 780 entries from 2000–2005. Notably, the preparation of monodispersed magnetic nanoparticles is (almost) improved to perfection. Although the impetus for making magnetic nanoparticles originally was to find materials suitable for ultrahigh-density magnetic storage media, the application of magnetic nanoparticles has begun to show remarkable promise in other industrial sectors including biotechnology and biomedicine. Biofunctional (or biofunctionalized) magnetic nanoparticles are gaining importance in solving both fundamental and practical problems in life sciences.

In terms of the studies on biofunctional magnetic nanoparticles, there are several interesting challenges that are yet to be met. First, we need a robust surface chemistry to attach bioactive molecules onto magnetic nanoparticles without laborious synthetic efforts. Second, we need more precise control of the numbers and orientations of the molecules on the surfaces of magnetic nanoparticles. Third, we need multifunctional and (perhaps) multimodal magnetic nanoparticles for biological applications. We anticipate that collaborative efforts of researchers from several disciplines will enable and advance the applications of biofunctional magnetic nanoparticles.

Acknowledgements

This work was partially supported by RGC (Hong Kong), EHIA (HKUST) and a DuPont Young Faculty Grant. B. X. thanks P. L. Ho, X. X. Zhang, Z. H. Guo, and C. K. Chang.

References

1 S. H. Sun, C. B. Murray, D. Weller, L. Folks and A. Moser, *Science*, 2000, **287**, 1989.
2 S. H. Sun and H. Zeng, *J. Am. Chem. Soc.*, 2002, **124**, 8204; T. Hyeon, *Chem. Commun.*, 2003, 927.
3 S. H. Sun, H. Zeng, D. B. Robinson, S. Raoux, P. M. Rice, S. X. Wang and G. X. Li, *J. Am. Chem. Soc.*, 2004, **126**, 273; S. J. Park, S. Kim, S. Lee, Z. G. Khim, K. Char and T. Hyeon, *J. Am. Chem. Soc.*, 2000, **122**, 8581; T. Hyeon, S. S. Lee, J. Park, Y. Chung and H. Bin Na, *J. Am. Chem. Soc.*, 2001, **123**, 12798; J. Joo, H. B. Na, T. Yu, J. H. Yu, Y. W. Kim, F. X. Wu, J. Z. Zhang and T. Hyeon, *J. Am. Chem. Soc.*, 2003, **125**, 11100; V. F. Puntes, K. M. Krishnan and A. P. Alivisatos, *Science*, 2001, **291**, 2115; V. F. Puntes, D. Zanchet, C. K. Erdonmez and A. P. Alivisatos, *J. Am. Chem. Soc.*, 2002, **124**, 12874.
4 S. G. Grancharov, H. Zeng, S. H. Sun, S. X. Wang, S. O'Brien, C. B. Murray, J. R. Kirtley and G. A. Held, *J. Phys. Chem. B*, 2005, **109**, 13030; S. X. Wang, S. Y. Bae, G. X. Li, S. H. Sun, R. L. White, J. T. Kemp and C. D. Webb, *J. Magn. Magn. Mater.*, 2005, **293**, 731; Y. G. Sun and Y. N. Xia, *Science*, 2002, **298**, 2176; Y. N. Xia, B. Gates, Y. D. Yin and Y. Lu, *Adv. Mater.*, 2000, **12**, 693; C. B. Murray, D. J. Norris and M. G. Bawendi, *J. Am. Chem. Soc.*, 1993, **115**, 8706; C. B. Murray, C. R. Kagan and M. G. Bawendi, *Science*, 1995, **270**, 1335; M. Nirmal, B. O. Dabbousi, M. G. Bawendi, J. J. Macklin, J. K. Trautman, T. D. Harris and L. E. Brus, *Nature*, 1996, **383**, 802; H. Mattoussi,

J. M. Mauro, E. R. Goldman, G. P. Anderson, V. C. Sundar, F. V. Mikulec and M. G. Bawendi, *J. Am. Chem. Soc.*, 2000, **122**, 12142; F. V. Mikulec, M. Kuno, M. Bennati, D. A. Hall, R. G. Griffin and M. G. Bawendi, *J. Am. Chem. Soc.*, 2000, **122**, 2532; S. Kim, Y. T. Lim, E. G. Soltesz, A. M. De Grand, J. Lee, A. Nakayama, J. A. Parker, T. Mihaljevic, R. G. Laurence, D. M. Dor, L. H. Cohn, M. G. Bawendi and J. V. Frangioni, *Nat. Biotechnol.*, 2004, **22**, 93; C. A. Mirkin, R. L. Letsinger, R. C. Mucic and J. J. Storhoff, *Nature*, 1996, **382**, 607; X. G. Peng, L. Manna, W. D. Yang, J. Wickham, E. Scher, A. Kadavanich and A. P. Alivisatos, *Nature*, 2000, **404**, 59; A. P. Alivisatos, *Science*, 1996, **271**, 933; M. Bruchez, M. Moronne, P. Gin, S. Weiss and A. P. Alivisatos, *Science*, 1998, **281**, 2013; B. Zhang, C. Cao, X. Xiang and H. Zhu, *Chem. Commun.*, 2004, 2452; G. M. Whitesides, *Small*, 2005, **1**, 172; S. Rozhok, C. K.-F. Shen, P.-L. H. Littler, Z. Fan, C. Liu, C. A. Mirkin and R. C. Holz, *Small*, 2005, **1**, 445; T. Pellegrino, S. Kudera, T. Liedl, A. M. Javier, L. Manna and W. J. Parak, *Small*, 2005, **1**, 48; Z. W. Pan, Z. R. Dai and Z. L. Wang, *Science*, 2001, **291**, 1947; C. Mao, D. J. Solis, B. D. Reiss, S. T. Kottmann, R. Y. Sweeney, A. Hayhurst, G. Georgiou, B. Iverson and A. M. Belcher, *Science*, 2004, **303**, 213; X.-S. Fang, C.-H. Ye, L.-D. Zhang and T. Xie, *Adv. Mater.*, 2005, **17**, 1661; X. S. Fang, C. H. Ye, L. D. Zhang, Y. H. Wang and Y. C. Wu, *Adv. Funct. Mater.*, 2005, **15**, 63; X. S. Fang, C. H. Ye, X. S. Peng, Y. H. Wang, Y. C. Wu and L. D. Zhang, *J. Mater. Chem.*, 2003, **13**, 3040.

5 H. W. Gu, R. K. Zheng, X. X. Zhang and B. Xu, *J. Am. Chem. Soc.*, 2004, **126**, 5664.

6 H. W. Gu, B. Xu, J. C. Rao, R. K. Zheng, X. X. Zhang, K. K. Fung and C. Y. C. Wong, *J. Appl. Phys.*, 2003, **93**, 7589.

7 H. W. Gu, Z. M. Yang, J. H. Gao, C. K. Chang and B. Xu, *J. Am. Chem. Soc.*, 2005, **127**, 34.

8 I. L. Medintz, H. T. Uyeda, E. R. Goldman and H. Mattoussi, *Nat. Mater.*, 2005, **4**, 435; X. H. Gao, L. L. Yang, J. A. Petros, F. F. Marshal, J. W. Simons and S. M. Nie, *Curr. Opin. Biotechnol.*, 2005, **16**, 63; A. M. Smith, X. H. Gao and S. M. Nie, *Photochem. Photobiol.*, 2004, **80**, 377; H. W. Gu, K. M. Xu, Z. M. Yang, C. K. Chang and B. Xu, *Chem. Commun.*, 2005, 4270.

9 A. Verma and V. M. Rotello, *Chem. Commun.*, 2005, 303; R. Elghanian, J. J. Storhoff, R. C. Mucic, R. L. Letsinger and C. A. Mirkin, *Science*, 1997, **277**, 1078; J. J. Storhoff, R. Elghanian, R. C. Mucic, C. A. Mirkin and R. L. Letsinger, *J. Am. Chem. Soc.*, 1998, **120**, 1959; T. A. Taton, C. A. Mirkin and R. L. Letsinger, *Science*, 2000, **289**, 1757; S. J. Park, T. A. Taton and C. A. Mirkin, *Science*, 2002, **295**, 1503; N. L. Rosi and C. A. Mirkin, *Chem. Rev.*, 2005, **105**, 1547.

10 S. M. Nie, D. T. Chiu and R. N. Zare, *Science*, 1994, **266**, 1018; S. M. Nie and S. R. Emery, *Science*, 1997, **275**, 1102; W. C. W. Chan and S. M. Nie, *Science*, 1998, **281**, 2016; W. C. W. Chan, D. J. Maxwell, X. H. Gao, R. E. Bailey, M. Y. Han and S. M. Nie, *Curr. Opin. Biotechnol.*, 2002, **13**, 40; X. H. Gao, Y. Y. Cui, R. M. Levenson, L. W. K. Chung and S. M. Nie, *Nat. Biotechnol.*, 2004, **22**, 969.

11 J. I. Park, M. G. Kim, Y. W. Jun, J. S. Lee, W. R. Lee and J. Cheon, *J. Am. Chem. Soc.*, 2004, **126**, 9072; J. I. Park and J. Cheon, *J. Am. Chem. Soc.*, 2001, **123**, 5743; L. E. M. Howard, H. L. Nguyen, S. R. Giblin, B. K. Tanner, I. Terry, A. K. Hughes and J. S. O. Evans, *J. Am. Chem. Soc.*, 2005, **127**, 10140.

12 J. M. Perez, F. J. Simeone, A. Tsourkas, L. Josephson and R. Weissleder, *Nano Lett.*, 2004, **4**, 119; J. Grimm, J. M. Perez, L. Josephson and R. Weissleder, *Cancer Res.*, 2004, **64**, 639; J. M. Perez, F. J. Simeone, Y. Saeki, L. Josephson and R. Weissleder, *J. Am. Chem. Soc.*, 2003, **125**, 10192; J. M. Perez, T. O'Loughin, F. J. Simeone, R. Weissleder and L. Josephson, *J. Am. Chem. Soc.*, 2002, **124**, 2856; J. M. Perez, L. Josephson, T. O'Loughlin, D. Hogemann and R. Weissleder, *Nat. Biotechnol.*, 2002, **20**, 816.

13 Y. M. Huh, Y. W. Jun, H. T. Song, S. Kim, J. S. Choi, J. H. Lee, S. Yoon, K. S. Kim, J. S. Shin, J. S. Suh and J. Cheon, *J. Am. Chem. Soc.*, 2005, **127**, 12387; H. T. Song, J. S. Choi, Y. M. Huh, S. Kim, Y. W. Jun, J. S. Suh and J. Cheon, *J. Am. Chem. Soc.*, 2005, **127**, 9992; Y. W. Jun, Y. M. Huh, J. S. Choi, J. H. Lee, H. T. Song, S. Kim, S. Yoon, K. S. Kim, J. S. Shin, J. S. Suh and J. Cheon, *J. Am. Chem. Soc.*, 2005, **127**, 5732.

14 E. Katz and I. Willner, *Chem. Commun.*, 2005, 4089; E. Katz, O. Lioubashevski and I. Willner, *J. Am. Chem. Soc.*, 2004, **126**, 11088; Y. Weizmann, F. Patolsky, O. Lioubashevski and I. Willner, *J. Am. Chem. Soc.*, 2004, **126**, 1073; Y. Weizmann, F. Patolsky, E. Katz and I. Willner, *J. Am. Chem. Soc.*, 2003, **125**, 3452.

15 K. J. Dormer, N. A. Kotov and C. E. Seeney, *FASEB J.*, 2003, **17**, A144; N. N. Mamedova, N. A. Kotov, A. L. Rogach and J. Studer, *Nano Lett.*, 2001, **1**, 281; T. J. Yoon, J. S. Kim, B. G. Kim, K. N. Yu, M. H. Cho and J. K. Lee, *Angew. Chem., Int. Ed.*, 2005, **44**, 1068.

16 A. K. Gupta and M. Gupta, *Biomaterials*, 2005, **26**, 3995; S. Mornet, S. Vasseur, F. Grasset and E. Duguet, *J. Mater. Chem.*, 2004, **14**, 2161; Q. A. Pankhurst, J. Connolly, S. K. Jones and J. Dobson, *J. Phys. D: Appl. Phys.*, 2003, **36**, R167.

17 H. W. Gu, P. L. Ho, K. W. T. Tsang, L. Wang and B. Xu, *J. Am. Chem. Soc.*, 2003, **125**, 15702.

18 H. W. Gu, P. L. Ho, K. W. T. Tsang, C. W. Yu and B. Xu, *Chem. Commun.*, 2003, 1966.

19 C. J. Xu, K. M. Xu, H. W. Gu, R. K. Zheng, H. Liu, X. X. Zhang, Z. H. Guo and B. Xu, *J. Am. Chem. Soc.*, 2004, **126**, 9938.

20 C. J. Xu, K. M. Xu, H. W. Gu, X. F. Zhong, Z. H. Guo, R. K. Zheng, X. X. Zhang and B. Xu, *J. Am. Chem. Soc.*, 2004, **126**, 3392.

21 D. Weller and A. Moser, *IEEE Trans. Magn.*, 1999, **35**, 4423.

22 K. C. Ho, P. J. Tsai, Y. S. Lin and Y. C. Chen, *Anal. Chem.*, 2004, **76**, 7162; Y. S. Lin, P. J. Tsai, M. F. Weng and Y. C. Chen, *Anal. Chem.*, 2005, **77**, 1753.

23 H. W. Gu, P. L. Ho, E. Tong, L. Wang and B. Xu, *Nano Lett.*, 2003, **3**, 1261.

24 J. M. Abad, S. F. L. Mertens, M. Pita, V. M. Fernandez and D. J. Schiffrin, *J. Am. Chem. Soc.*, 2005, **127**, 5689.

25 L. X. Chen, T. Liu, M. C. Thurnauer, R. Csencsits and T. Rajh, *J. Phys. Chem. B*, 2002, **106**, 8539.

26 R. Hong, N. O. Fischer, T. Emrick and V. M. Rotello, *Chem. Mater.*, 2005, **17**, 4617.

27 U. N. Sundram, J. H. Griffin and T. I. Nicas, *J. Am. Chem. Soc.*, 1996, **118**, 13107.

28 B. G. Xing, P. L. Ho, C. W. Yu, K. H. Chow, H. W. Gu and B. Xu, *Chem. Commun.*, 2003, 2224; B. G. Xing, C. W. Yu, P. L. Ho, K. H. Chow, T. Cheung, H. W. Gu, Z. W. Cai and B. Xu, *J. Med. Chem.*, 2003, **46**, 4904; L. H. Li and B. Xu, *Curr. Pharm. Des.*, 2005, **11**, 3111.

29 A. Campion and P. Kambhampati, *Chem. Soc. Rev.*, 1998, **27**, 241.

30 A. D. Dinsmore, M. F. Hsu, M. G. Nikolaides, M. Marquez, A. R. Bausch and D. A. Weitz, *Science*, 2002, **298**, 1006.